



# Uptake of L-Alanine and Its Distinct Roles in the Bioenergetics of *Trypanosoma cruzi*

Richard M. B. M. Girard,<sup>a</sup> Marcell Crispim,<sup>a</sup> Mayke Bezerra Alencar,<sup>a</sup> Ariel Mariano Silber<sup>a</sup>

<sup>a</sup>Department of Parasitology, Laboratory of Biochemistry of Tryps - LaBTryps, Institute of Biomedical Sciences, University of São Paulo, Cidade Universitária, Butantã, São Paulo, São Paulo, Brazil

**ABSTRACT** Amino acids participate in several critical processes in the biology of trypanosomatids, such as osmoregulation, cell differentiation, and host cell invasion. Some of them provide reducing power for mitochondrial ATP synthesis. It was previously shown that alanine, which is formed mainly by the amination of pyruvate, is a metabolic end product formed when parasites are replicating in a medium rich in glucose and amino acids. It was shown as well that this amino acid can also be used for the regulation of cell volume and resistance to osmotic stress. In this work, we demonstrate that, despite it being an end product of its metabolism, *Trypanosoma cruzi* can take up and metabolize L-Ala through a low-specificity nonstereoselective active transport system. The uptake was dependent on the temperature in the range between 10 and 40°C, which allowed us to calculate an activation energy of 66.4 kJ/mol and estimate the number of transporters per cell at ~436,000. We show as well that, once taken up by the cells, L-Ala can be completely oxidized to CO<sub>2</sub>, supplying electrons to the electron transport chain, maintaining the electrochemical proton gradient across the mitochondrial inner membrane, and supporting ATP synthesis in *T. cruzi* epimastigotes. Our data demonstrate a dual role for Ala in the parasite's bioenergetics, by being a secreted end product of glucose catabolism and taken up as nutrient for oxidative mitochondrial metabolism.

**IMPORTANCE** It is well known that trypanosomatids such as the etiological agent of Chagas' disease, *Trypanosoma cruzi*, produce alanine as a main end product of their energy metabolism when they grow in a medium containing glucose and amino acids. In this work, we investigated if under starvation conditions (which happen during the parasite life cycle) the secreted alanine could be recovered from the extracellular medium and used as an energy source. Herein we show that indeed, in parasites submitted to metabolic stress, this metabolite can be taken up and used as an energy source for ATP synthesis, allowing the parasite to extend its survival under starvation conditions. The obtained results point to a dual role for Ala in the parasite's bioenergetics, by being a secreted end product of glucose catabolism and taken up as nutrient for oxidative mitochondrial metabolism.

**KEYWORDS** Chagas disease, L-alanine metabolism, L-alanine uptake, *Trypanosoma cruzi*, bioenergetics

*Trypanosoma cruzi*, the etiological agent of Chagas' disease or American trypanosomiasis, is a quite unique organism in terms of its metabolism and bioenergetics (1, 2). This protist experiences a myriad of environmental conditions during its complex life cycle, which occur inside the entire digestive tube of triatomine insect vectors, the blood of more than 100 species of mammals, and the cytosol of (potentially) every mammalian nucleated cell in every tissue and organ (3). As a consequence of its transit through all these different environments, *T. cruzi* faces different conditions, varying in terms of the availability of nutrients, especially inside the insect vector, where *T. cruzi*

Received 21 June 2018 Accepted 22 June 2018 Published 18 July 2018

**Citation** Girard RMBM, Crispim M, Alencar MB, Silber AM. 2018. Uptake of L-alanine and its distinct roles in the bioenergetics of *Trypanosoma cruzi*. mSphere 3:e00338-18. <https://doi.org/10.1128/mSphereDirect.00338-18>.


**Editor** Ira J. Blader, University at Buffalo

**Copyright** © 2018 Girard et al. This is an open-access article distributed under the terms of the [Creative Commons Attribution 4.0 International license](https://creativecommons.org/licenses/by/4.0/).

Address correspondence to Ariel Mariano Silber, [asilber@usp.br](mailto:asilber@usp.br).

Solicited external reviewers: Richard Burchmore, University of Glasgow; Achim Schnauffer, University of Edinburgh; Roberto Docampo, University of Georgia.

This paper was submitted via the [mSphereDirect™ pathway](https://msphere.direct).

 L-alanine as a metabolic waste and a "fuel for life" in the bioenergetics of *Trypanosoma cruzi*. @Ariel\_Lab

could be confronted by severe nutritional stress (4, 5). Therefore, *T. cruzi* has to be equipped with a set of transporters and enzymes able to take up and metabolize the metabolites available in each one of these environments (2, 6). Among such different metabolites, it was consistently shown that several amino acids can be used as an energy source: Pro, Asp, His, Glu, Asn, Gln, Leu, and Ile (1, 6–14). Beyond their role in the parasite bioenergetics and protein synthesis, amino acids are involved in various critical biological functions in *T. cruzi*, such as cell differentiation, resistance to different forms of oxidative stress and starvation, infection of the mammalian host cells, and proliferation in the intracellular environment (2, 11, 12, 15, 16).

Ala, together with succinate, is one of the end products of the metabolism of glucose by epimastigotes, the parasite's form living in the digestive tube of the insect vector, and as such, the main intracellular and secreted amino acid (17–19). Ala is the product of the reversible amination of pyruvate. Under conditions of excess of  $\text{NH}_4^+$ , Ala can be produced through an Ala dehydrogenase or the concerted action of an NAD-linked Glu dehydrogenase and aminotransferases that accept pyruvate as a substrate (20–23). Thus, Ala production might be also linked to reoxidation of glycolytically produced NADH, even under aerobic conditions (17, 24, 25). Interestingly, both intracellular and secreted pools of Ala are produced separately and were shown to be compartmentalized (18). Notably, early studies suggested that, despite being an end product of the metabolism, Ala can be metabolized by *T. cruzi* since it was able to trigger  $\text{O}_2$  consumption (10). Indeed, depending on the relative quantity of substrates and products, Ala could be reconverted into pyruvate by the same aminotransferases or Ala dehydrogenases that produce it (20, 25).

Another relevant role involving formation, influx, and efflux of Ala is its participation as part of the response to osmotic stress in *T. cruzi* (26–28). Notwithstanding its biological significance, Ala uptake and oxidation have not yet been characterized in *T. cruzi*. In this work, we biochemically describe in this organism a single Ala transport system as well as the mitochondrial oxidation of the amino acid through the evaluation of bioenergetics parameters. Ala, a multifunctional metabolite, depending on the metabolic conditions, can be a metabolic end product or can be a substrate to feed electrons into the respiratory chain for ATP production.

## RESULTS

**L-Ala uptake in *T. cruzi* epimastigotes.** To characterize the L-Ala transport system, we initially performed a time course assay for the uptake of L-Ala at a presumably saturating substrate concentration. For this, we incubated the parasites in the presence of 5 mM L-Ala and monitored the internalization of the amino acid over time. The obtained data could be fitted by an exponential decay function ( $r^2 = 0.97$ ), as expected for the uptake of metabolites mediated by a transport system (Fig. 1A). Given that the transported L-Ala increased in an approximately linear way for up to 3 min ( $r^2 = 0.96$  [Fig. 1A, inset]) the incubation time to measure the initial velocity ( $V_0$ ) of L-Ala transport was set to 1 min. In order to calculate the kinetic parameters of the L-Ala uptake process,  $V_0$  was measured as a function of the L-Ala extracellular concentration. A classical Michaelis-Menten hyperbolic function approached the data ( $r^2 = 0.89$ ), allowing the calculation of both kinetic parameters  $V_{\text{max}}$  and  $K_m$ , which were  $1.86 \pm 0.3 \text{ nmol}\cdot\text{min}^{-1}$  per  $20 \times 10^6$  cells and  $1.81 \text{ } 0.6 \pm \text{ mM}$ , respectively (Fig. 1B; see Fig. S1 and Table S1 in the supplemental material).

To determine the transporter specificity, we evaluated the ability of other amino acids as competitors. Short-chain amino acids, such as L-Gly and L-Ser, strongly inhibited L-Ala transport (inhibition of 76% and 84%, respectively). L-Cys and L-Pro also inhibited the L-Ala uptake by the cells, but to a lesser extent (inhibition of 53% and 33%, respectively). Remarkably, a 10-fold excess of D-Ala inhibited L-Ala uptake by 43.7%. All other amino acids tested as possible competitors of L-Ala uptake showed only a weak inhibition pattern if any (Table 1).

**Thermodynamic analysis of L-Ala transport.** The effect of temperature on L-Ala uptake was evaluated by measuring  $V_{\text{max}}$  (assuming that  $V_{\text{max}}$  is equivalent to  $V_0$  at a

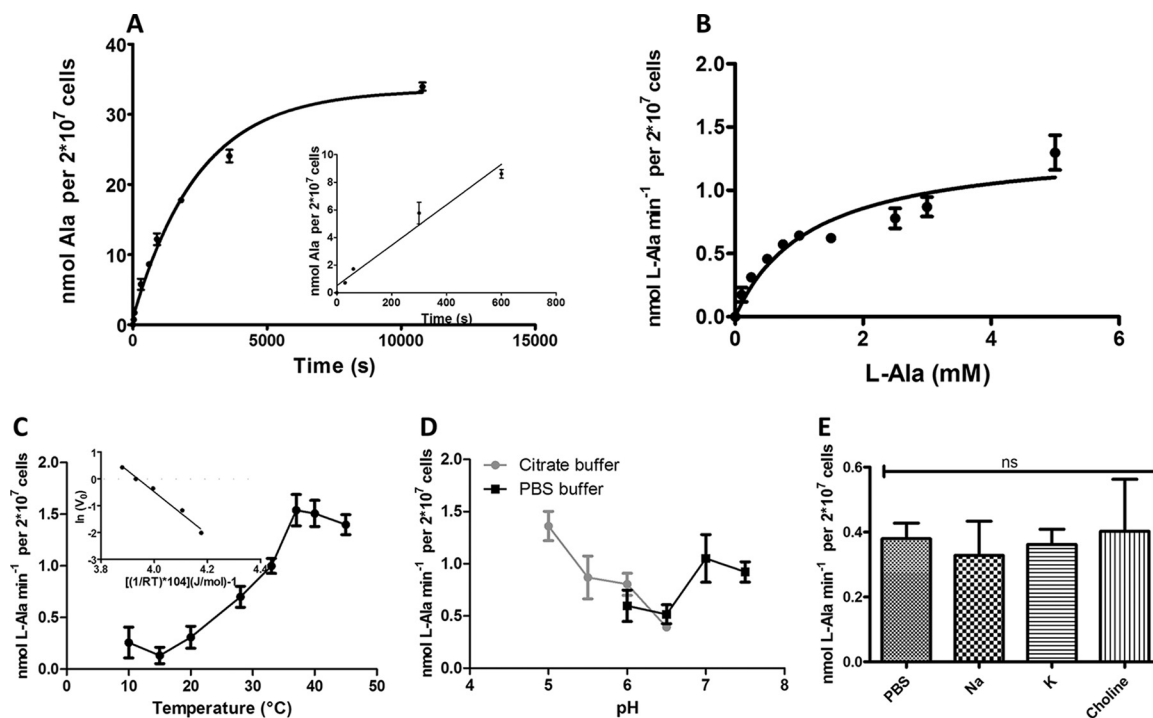


**FIG 1** L-Ala uptake characterization. (A) Time course of L-Ala incorporation by the epimastigotes of *Trypanosoma cruzi*. The incorporation of 5 mM L-Ala traced with a radiolabeled amino acid was followed up as described in Materials and Methods. (Inset) L-Alanine was incorporated into the cells in a nearly linear manner for 3 min. All of the assays were performed in technical triplicate, and the data correspond to a representative of four independent biological experiments. (B) Effect of L-alanine concentration on L-Ala uptake as described in Materials and Methods. All of the assays were performed in technical triplicate, and the data correspond to a representative of four independent biological experiments. (C) Effect of temperature on L-Ala uptake. Epimastigotes of *T. cruzi* were incubated in the presence of L-Ala at different temperatures ranging between 10 and 45°C, and the  $V_0$  was measured. (Inset) Arrhenius plot from which the apparent energy of activation ( $E_a$ ) and Arrhenius constant (A) were calculated. All of the assays were performed in technical triplicate, and the data correspond to mean values from four independent biological experiments. (D) pH dependence of L-Ala transport in epimastigotes of *T. cruzi*.  $V_0$  was measured at pH values ranging between 5.0 and 7.5. For the range of pH values between 5.0 and 6.5, citrate buffer was used, whereas for the range of pH values between 6 and 7.5, PBS buffer was used. All of the assays were performed in technical triplicate, and the data correspond to a representative of three independent biological experiments. (E) The effect of cations Na<sup>+</sup> and K<sup>+</sup> on L-Ala transport.  $V_0$  was measured in cells resuspended in PBS (145 mM Na<sup>+</sup> and 4.5 mM K<sup>+</sup>) or in phosphate buffers containing only Na<sup>+</sup> (149.5 mM) or K<sup>+</sup> (149.5 mM) as cations. Choline (139.7 mM) was used as the control. These data were analyzed using one-way analysis of variance (ANOVA) and Tukey's posttest. No statistical differences (ns) were observed at  $P < 0.05$ .

saturation L-Ala concentration [5 mM]) at temperatures ranging from 10 to 45°C. As expected, an exponential increase of  $V_0$  was observed as a function of the temperature between 15 and 37°C, while in the range of 40 to 45°C, no velocity increases were observed (Fig. 1C). The changes in  $V_0$  in the exponential region of the curve were used to compute  $Q_{10}$ , which was 2.47.  $Q_{10}$  is the ratio of the velocity of a reaction at a given temperature to that of the same reaction at a temperature 10°C lower. The invariant  $V_0$  value obtained for temperatures above 40°C can be attributed to the fact that temperature-dependent protein denaturation would be compensating any increase in

**TABLE 1** Percentage of inhibition of L-Ala uptake when the transport assay was performed with parasites in the presence of 10-fold excess of competitor amino acid

Competitor	% of L-Ala uptake inhibition
D-Alanine	44.9 ± 3.5
Glycine	76 ± 10
Serine	84 ± 7.5
Cysteine	53 ± 9
Proline	33 ± 8.2
Aspartate	10 ± 7.4
Glutamate	10 ± 1.7
Glutamine	9.5 ± 7.4

**TABLE 2** Effect of oligomycin A and FCCP on L-Ala uptake in *Trypanosoma cruzi* epimastigotes

Addition(s)	% of L-Ala uptake inhibition
Control	0
Oligomycin A (5 $\mu\text{g/ml}$ )	
0 min	4.2 $\pm$ 7.9
30 min	48.6 $\pm$ 8.8
FCCP (0.5 $\mu\text{M}$ )	44.2 $\pm$ 11
Oligomycin A (5 $\mu\text{g/ml}$ ) + FCCP (0.5 $\mu\text{M}$ )	53.4 $\pm$ 9.9

activity. The  $V_0$  measurements made between 15 and 37°C were also used to calculate the energy of activation ( $E_a$ ) from an Arrhenius plot, which resulted to be 66.4  $\pm$  9 kJ/mol (Fig. 1C, inset). Additionally, from the Arrhenius equation, it was possible to calculate the approximate number of transporters being used for the substrate uptake. The value 1.38 attomol per cell (see Text S1 in the supplemental material) could be estimated, which would be equivalent to approximately  $4.36 \times 10^5$  transporters per cell.

**External ion sensitivity and driving force of L-Ala uptake.** To advance the biochemical characterization of the L-Ala transporter, we were interested in measuring the influence of  $\text{H}^+$ ,  $\text{Na}^+$ , and  $\text{K}^+$  on its uptake. The  $\text{H}^+$  dependence of L-Ala uptake was analyzed by measuring  $V_0$  at different pH values in the range from 5 to 7.5. Our data exhibited a maximum value for  $V_0$  at pH 5.0, with a sharp decrease in the range between 6.0 and 6.5. Interestingly, at pH values between 7.0 and 7.5, we observed a significant increase, reaching levels close to those observed at an acidic pH (Fig. 1D). Next, we evaluated the effect of  $\text{Na}^+$  and  $\text{K}^+$  on L-Ala uptake. The transport was measured in modified phosphate-buffered saline (PBS) buffers, enriched in  $\text{Na}^+$  ( $\text{K}^+$  excluded), in  $\text{K}^+$  ( $\text{Na}^+$  excluded), regular PBS, or PBS in which the ionic strength was adjusted with choline (avoiding supplementation with  $\text{Na}^+$  or  $\text{K}^+$ ). None of the conditions affected L-Ala uptake (Fig. 1E).

To determine if L-Ala uptake involves active transport, the influence of the intracellular ATP levels on  $V_0$  was initially evaluated. For this, L-Ala transport was measured in parasites previously incubated for 30 min with 5  $\mu\text{g/ml}$  oligomycin A or not (with a control, where the oligomycin is added without preincubation, to assess if this ATP synthase inhibitor does not have an off-target effect on the transport system), as it was previously demonstrated that this 30-min treatment decreases the intracellular ATP levels by 60%, while without preincubation, it did not affect the ATP levels (29, 30). The fact that we observed a significant diminution of L-Ala uptake (48.6%  $\pm$  8.8%) only in parasites preincubated for 30 min with oligomycin A indicates that this is an active process (Table 2). In addition, L-Ala uptake was decreased in the presence of carbonyl cyanide *p*-trifluoromethoxyphenylhydrazone (FCCP) alone (44.2%  $\pm$  11.1%), which supports the possibility of transport being dependent on an  $\text{H}^+$  gradient across the plasma membrane as the driving force (31). However, it is known that FCCP, as an uncoupler, collapses the mitochondrial inner membrane potential ( $\Delta\Psi_m$ ), and as a response to this, the  $\text{F}_1\text{F}_0$  ATP-synthase could start to work in “reverse mode” (32), hydrolyzing ATP to pump protons to the intermembrane mitochondrial space. Thus, FCCP treatment triggers in fact at least two simultaneous effects: (i) the collapse of transmembrane proton gradients and (ii) the depletion of the intracellular ATP pools. To separate both effects, we measured the L-Ala uptake in cells simultaneously treated with FCCP and oligomycin A (without preincubation). The combined treatment impaired the L-Ala transport (53.4%  $\pm$  9.9%) (Table 2). In addition, L-Ala uptake was also assayed in the presence of carbonyl cyanide *m*-chlorophenylhydrazone (CCCP) at various concentrations (0, 10, 20, and 100  $\mu\text{M}$ ) to verify whether L-Ala can be incorporated in a transmembrane proton gradient-independent manner (see Fig. S2 in the supplemental material). Our data showed that 40% of L-Ala is incorporated at a high

concentration of H<sup>+</sup> gradient uncoupler. Taken together, these results indicate that L-Ala transport system is partially dependent on a transmembrane proton gradient as the driving force, which is maintained by plasma membrane P-type H<sup>+</sup>-ATPases (31).

**The bioenergetics of *T. cruzi* with L-Ala as the substrate.** To evaluate the role of L-Ala in the energy metabolism of *T. cruzi*, different bioenergetics parameters were evaluated. Initially, the viability of the parasites when incubated in PBS supplemented with this amino acid as the only energy source was evaluated and compared to the survival measured by supplementing PBS with other energy sources or not (controls). Thus, exponentially growing epimastigotes were incubated in PBS (negative control) or PBS supplemented with 5 mM L-Ala, 5 mM Pro, or 5 mM glucose. (The latter two are known energy sources for *T. cruzi* epimastigotes and therefore were used as positive controls.) After 24 and 48 h, cell viability was measured. The parasites incubated in L-Ala had their viability increased compared to those in nonsupplemented PBS (Fig. 2A) at both incubation times, suggesting that L-Ala can be metabolized as an energy source. In fact, once taken up by the cells, L-Ala can be converted into pyruvate by an Ala dehydrogenase, which is essentially glycosomal (25), or a transaminase accepting Ala as a substrate, such as the Tyr or Ala transaminases, which can be both mitochondrial and cytosolic (33). Then, pyruvate can be converted into malate by the cytosolic malic enzyme (34–37), and subsequently into fumarate or succinate, in the mitochondrion or glycosomes (38). Alternatively, pyruvate can be converted into acetyl coenzyme A (acetyl-CoA) through the pyruvate dehydrogenase complex (see Fig. 5) (20, 25). Whatever the case, at least part of the pyruvate may have as a final destiny its total oxidation to CO<sub>2</sub> plus H<sub>2</sub>O (39). In order to verify this possibility, epimastigotes were incubated for 30, 60, 240, and 300 min with L-[U-<sup>14</sup>C]Ala, and the time-dependent <sup>14</sup>CO<sub>2</sub> production was monitored (Fig. 2B). After a 60-min incubation, we observed that 10% of the transported amino acid was oxidized to CO<sub>2</sub>, while 65% of the detected radioactivity was incorporated into soluble metabolites, corresponding to free L-Ala and to the L-Ala eventually incorporated into other soluble macromolecules, and approximately 25% was incorporated into trichloroacetic acid-precipitable macromolecules (Table 3).

The ability of L-Ala to support ATP biosynthesis was also evaluated. Epimastigotes were subjected to a severe metabolic stress by incubating them for 30 h in PBS in the absence of any energy source. The cells were then evaluated for recovery of their ATP levels by incubating them for 1 h in the presence of 5 mM L-Ala, 5 mM Pro, or 5 mM His. Pro and His were positive controls since it was previously demonstrated that both are able to recover the intracellular ATP levels diminished by starvation (7, 40). A negative control consisting of keeping the parasites for 1 h in the absence of any metabolite was also performed. Then, intracellular ATP was measured by a luciferase assay. Parasites incubated in the presence of L-Ala showed a significant increase in the intracellular amounts of ATP compared to those in the negative control, and this increase was in the range of those obtained with Pro and His. Interestingly, the recovery of ATP levels was abolished by the addition of antimycin A (0.5 μM), a respiratory chain (complex III) inhibitor. These data strongly suggest that L-Ala can be used for fueling ATP synthesis through oxidative phosphorylation (Fig. 2C; see Fig. S3 in the supplemental material). As our results showed that L-Ala has a role in *T. cruzi* bioenergetics, we evaluated whether this amino acid is involved in maintaining the mitochondrial inner membrane potential ( $\Delta\Psi_m$ ). The cells were preincubated for 30 h in PBS buffer to induce a severe metabolic stress and then recovered by incubation for 1 h in 5 mM L-Ala in mitochondrial cellular respiration (MCR) buffer, 5 mM His in MCR buffer (positive control), or MCR buffer alone (negative control). Then, rhodamine 123, a fluorescent  $\Delta\Psi_m$  indicator was added, and the fluorescence measurements were made by cytometry (7). The degree of recovery of  $\Delta\Psi_m$  was calculated on the basis of the ratio of the fluorescence by cells not treated with FCCP (polarized mitochondrial membrane) and FCCP-treated (depolarized mitochondrial membrane) cells under each condition. The L-Ala-recovered cells restored their  $\Delta\Psi_m$  compared to the negative control, although the ability of this amino acid to restore  $\Delta\Psi_m$  was significantly lower than that of His

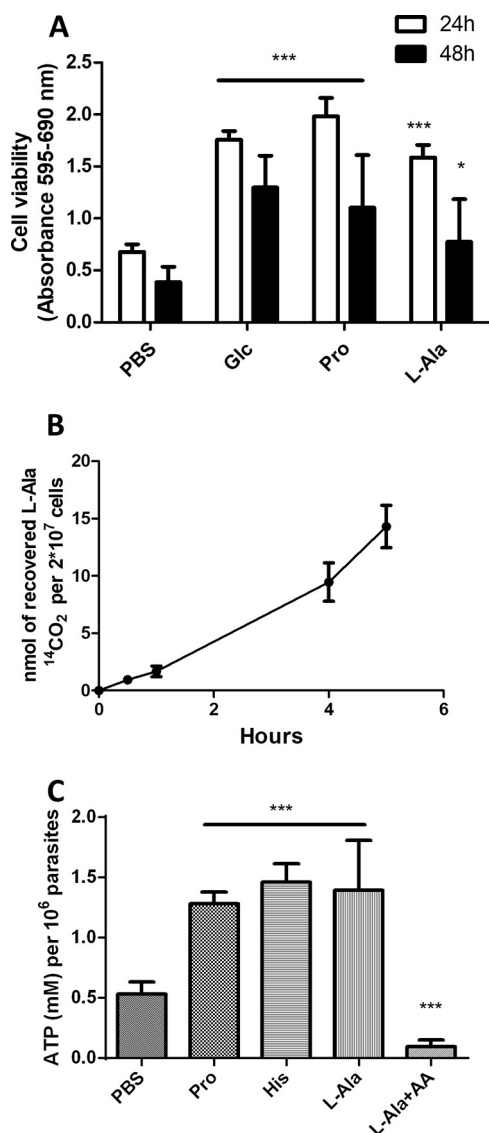


**FIG 2** The effect of L-Ala on bioenergetics parameters. (A) Viability assays of epimastigotes of *T. cruzi* using L-Ala as the only energy source. An MTT assay was used to assess epimastigotes in the exponential phase of growth (LIT medium) transferred to supplemented PBS. The viability was expressed as a percentage of formazan formation through the reduction of MTT with respect to the maximum viability obtained for this assay when cells were treated with Glc (glucose) or Pro (proline), both taken as positive controls. The parasites growing initially in LIT medium were transferred to supplemented PBS (or not [negative control]) with different substrates, including Glc and Pro as positive controls and were incubated for 24 or 48 h. Here, we consider the positive controls as viable parasite populations. (B)  $^{14}\text{CO}_2$  production from epimastigotes incubated in 5 mM L- $^{14}\text{C}$ Ala after 30, 60, 240, and 300 min. (C) ATP production from L-Ala catabolism. The intracellular ATP content after 60 min of recovery in parasites nutritionally stressed using the substrates indicated is shown. The ATP concentration was determined using a luciferase assay, and the data were normalized by the total cell number. AA, antimycin A (0.5  $\mu\text{M}$ ). One-way analysis of variance (ANOVA) followed by a Tukey's posttest was used for statistical analysis to compare the values to those from the respective control. \*\*\*,  $P < 0.001$ ; \*,  $P < 0.05$  (Tukey's posttest). Panels A, B, and C correspond to mean values from three independent biological experiments.

(Fig. 3C). As L-Ala was able to maintain the parasites' viability and sustain ATP production and the  $\Delta\Psi\text{m}$ , we also measured its ability to trigger parasite respiration. Epimastigotes were incubated for 16 h and then recovered with different substrates or not (basal respiration) for 30 min. His was used as positive control (7). The rates of  $\text{O}_2$  consumption were measured after the addition of cells, stimulated or not with L-Ala (basal respiration), then inhibited by the addition of oligomycin A, and finally uncoupled by FCCP to determine the leak of respiration and the maximum capacity of the

**TABLE 3** L-Ala incorporated in the soluble and insoluble fractions and <sup>14</sup>CO<sub>2</sub> produced from epimastigotes incubated in 5 mM L-[U-<sup>14</sup>C]Ala for 1 h

Fraction or CO <sub>2</sub>	L-[ <sup>14</sup> C]Ala incorporation or <sup>14</sup> CO <sub>2</sub> production (nmol/1 × 10 <sup>7</sup> cells)	% of L-Ala incorporation or <sup>14</sup> CO <sub>2</sub> production
Pellet	2.6 ± 0.39	24.7
Supernatant	6.9 ± 1.3	65.3
CO <sub>2</sub>	1.1 ± 0.5	10

electron transport system (ETS), respectively (Fig. 4). Our results demonstrate that, after 30 min of incubation, L-Ala triggered an O<sub>2</sub> consumption level that is similar to that recorded with His and higher than that of the nonstimulated parasites (Fig. 4). As expected, respiration rates triggered by L-Ala were inhibited by oligomycin A and then stimulated by FCCP, demonstrating its oxidation through the respiratory chain (Fig. 4D). Summarizing, our results show that L-Ala can deliver electrons to the respiratory chain and fuel ATP synthesis through oxidative phosphorylation in epimastigotes.

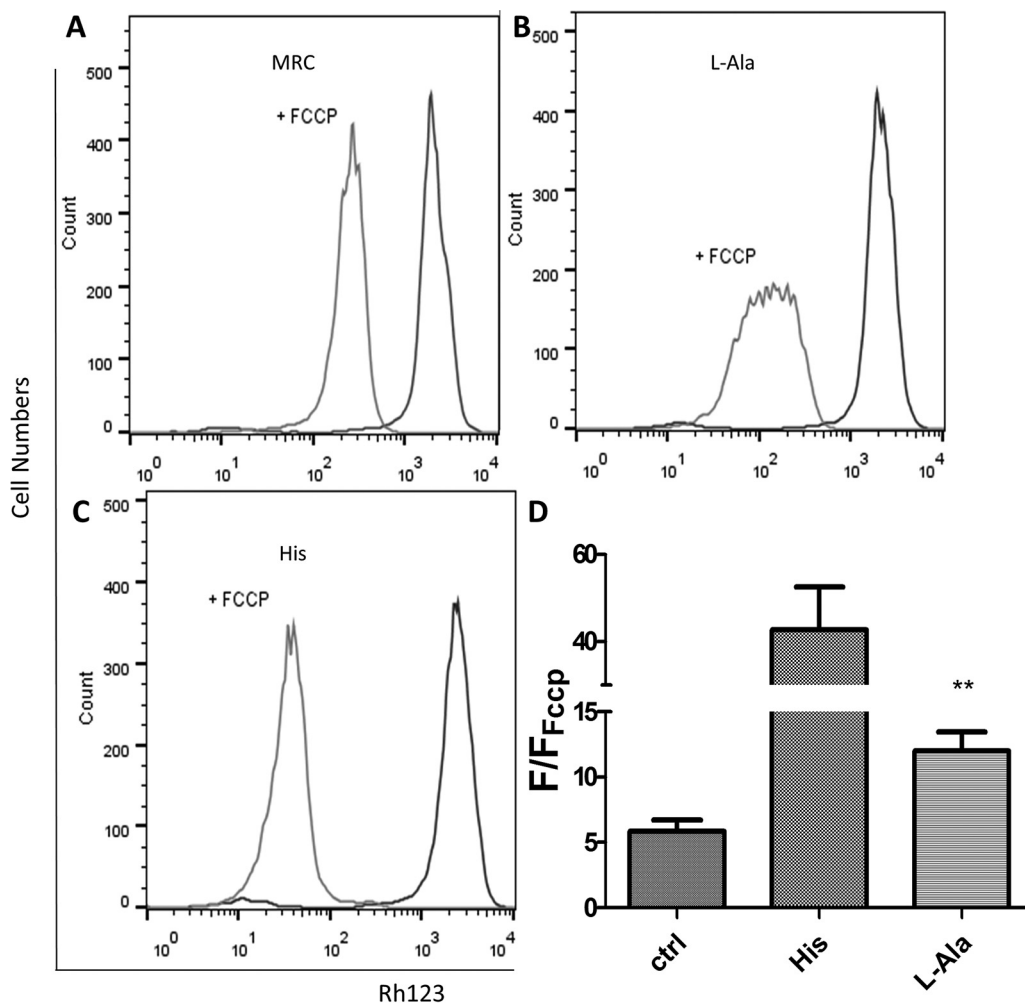


**FIG 3** Mitochondrial inner membrane potential by L-Ala catabolism. Flow cytometry analysis shows the fluorescence in epimastigotes incubated with rhodamine 123 after 30 h of nutritional stress and recovery or not (A) with L-Ala (B) or (C) His (C). “+ FCCP” indicates the fluorescence shift after the addition of the uncoupling agent. (D) The fluorescence ratios between the coupled and uncoupled parasites under each condition were calculated using the geometric mean (area under each peak). Samples were compared to the control using the *t* test. \*\*, *P* < 0.01. The data correspond to four independent biological experiments.

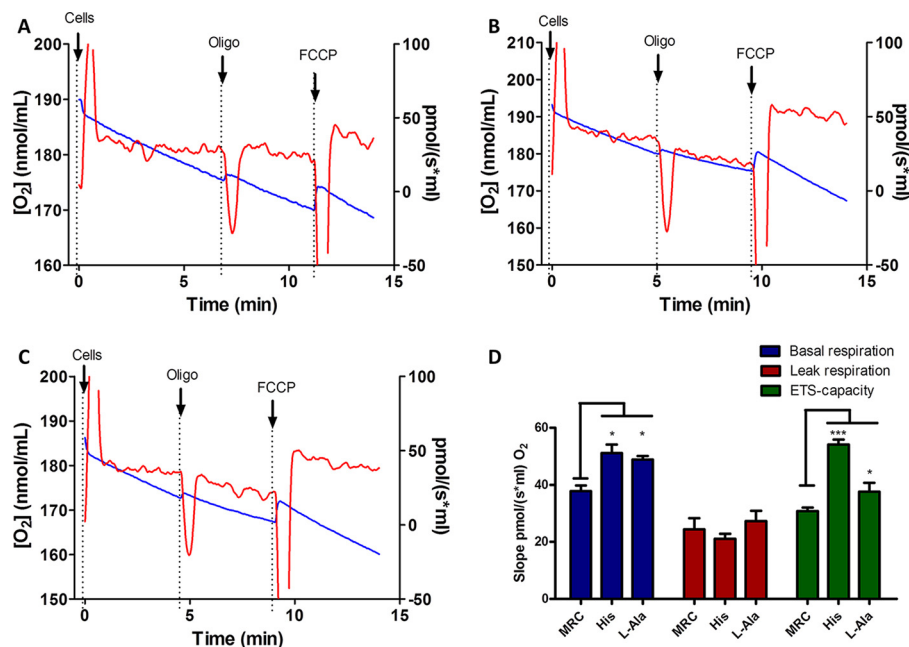


**FIG 4** Respiratory rates in recovered epimastigotes. Oxygen consumption was measured after starvation (16 h in PBS) without recovery (A) as a negative control and recovered by adding 5 mM His (B) for 30 min as a positive control or 5 mM L-Ala (C) for 30 min. The red lines indicate the variation in oxygen concentration as a function of time (right axis). The blue lines represent  $O_2$  concentration (left axis). Oligo, oligomycin A at 0.5  $\mu$ g/ml. FCCP was used at 0.5  $\mu$ M. (C) Basal respiration (initial oxygen flux values), leak respiration after the addition of 0.5  $\mu$ g/ml of oligomycin A, and electron transfer system (ETS) capacity after the addition of 0.5  $\mu$ M FCCP were measured for each condition. One-way ANOVA followed by a Tukey's posttest was used for statistical analysis to compare the values to the respective control. \*\*\*,  $P < 0.001$ ; \*,  $P < 0.05$  (Tukey's posttest). The data correspond to three independent biological experiments.

## DISCUSSION

Ala is available throughout *T. cruzi*'s life cycle. In the insect vector, this amino acid is present in both the hemolymph and the excreta (41–43). Ala is also available to the parasite forms when residing within the mammalian cells and in the plasma (44). Additionally, as mentioned, the parasite produces two independent pools of Ala as a consequence of its own metabolism (17, 18, 28, 33). These facts raise the importance of studying in more detail its uptake and subsequent metabolism.

Most of the biochemically characterized amino acid transport systems in *T. cruzi* showed functional characteristics that are compatible with those of members of the AAAP (amino acid/auxin permease) family, a family grouping  $H^+$ /amino acids and auxin permeases (45). Noteworthy, for *T. cruzi* the uptake of most of amino acids has already been biochemically analyzed (2).

In the present work, we biochemically described the uptake of L-Ala by *T. cruzi* epimastigotes. We identified a single transport system with a  $K_m$  similar to values already described for branched-chain amino acids (BCAAs),  $\gamma$ -aminobutyric acid (GABA), Glu, and Pro by transport system A. However, the  $V_{max}$  value is, to our knowledge, the highest reported until now for any amino acid transport system in *T. cruzi* (2). These data could in part explain the reported rapid changes in the concentration of intracellular Ala in cells under hyper- or hypo-osmotic stress (26–28). Such a function in osmoregulation was also attributed to the L-Ala transporters in *Leishmania* spp. (46–48).

Regarding the specificity, our results showed that amino acids structurally related to L-Ala, like short-chain amino acids (Ser and Gly), as well as neutral amino acids (Pro and Cys), compete with L-Ala for uptake. The transport activity increased exponentially at temperatures between 15 and 40°C, a range to which the parasites could be naturally exposed inside the insect vectors (49). Given this, we may assume that the environmental temperature is a natural modulator of L-Ala uptake. The obtained  $E_a$  was in the



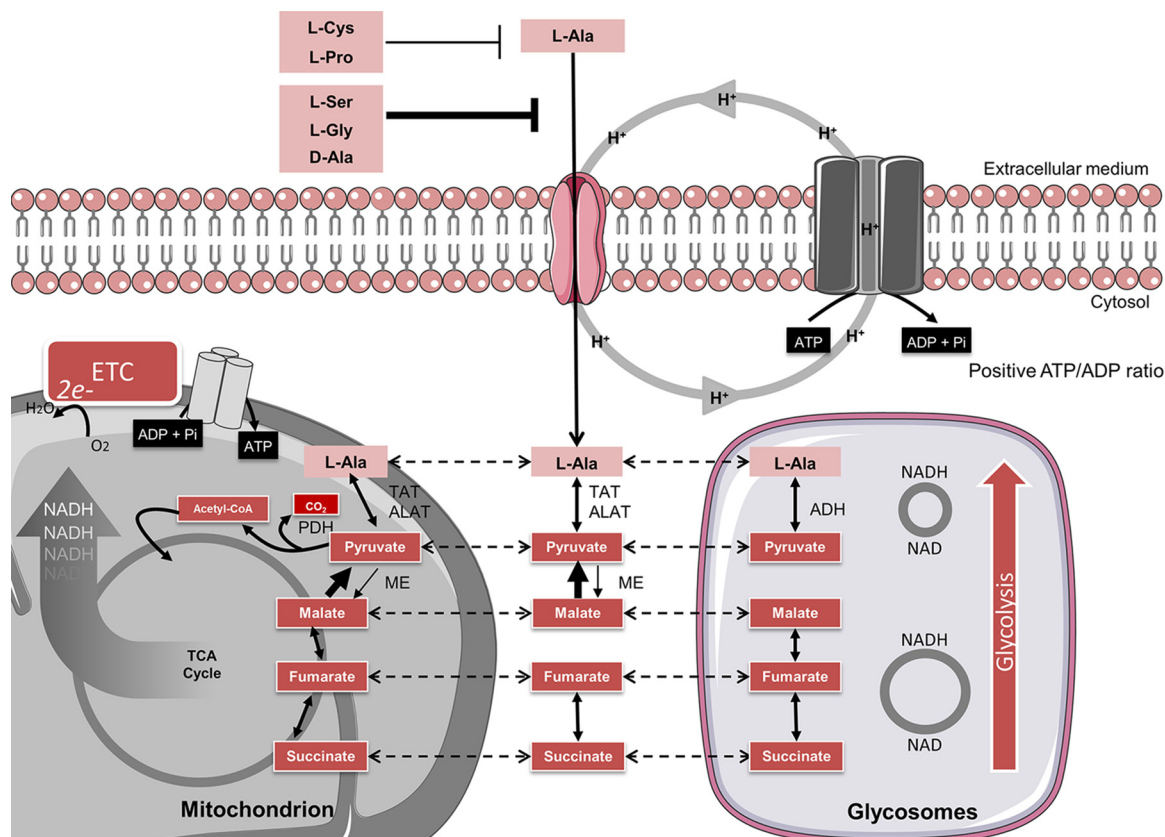


**FIG 5** Schematic proposal for the uptake and catabolism of L-Ala in *T. cruzi*. The glycosomal and mitochondrial compartments and the TCA cycle are indicated. The metabolic flux at each enzymatic step is represented by arrows of different thicknesses. Dashed arrows indicate the intracellular shuttle of the molecules between different compartments. ETC, electron transport chain; TAT, tyrosine aminotransferase; ALAT, Ala aminotransferase; ADH, Ala dehydrogenase; ME, malic enzyme; PDH, pyruvate dehydrogenase.

range of those reported for other amino acid transport systems, with the low-affinity Arg transporter as the only exception (30). Interestingly, the  $E_a$  corresponds approximately to a requirement for the hydrolysis of 2 molecules of ATP into ADP plus  $P_i$  per L-Ala molecule transported into the cells. Additionally, our data showed that L-Ala uptake is mediated by an active process and occurs similarly to that of L-Ala uptake in *Leishmania* and the transport of most amino acids in *T. cruzi* (2). The main driving force in these processes is a transmembrane  $H^+$  gradient, most likely created by a plasma membrane-located proton-pumping ATPase (Table 2; Fig. 5) (31).

As mentioned before, it has been well described that the *T. cruzi* epimastigotes' proliferation is initially based on the consumption of glucose (when available) and then, after the exhaustion of this metabolite, on the consumption of available amino acids (13, 17). As a consequence of the glucose consumption, the cells mainly produce succinate acetate and  $CO_2$  (50–52), while significant amounts of  $NH_4^+$  are produced when glucose is scarce (50, 53, 54), derived from the increased consumption of amino acids (7, 9, 13, 55). In *T. cruzi*, at least two systems have been proposed as being involved in the detoxification of the metabolically produced  $NH_4^+$  (56, 57). At the same time,  $NH_4^+$  can be used for NADH oxidation. This happens through the concerted action of (i) Glu dehydrogenases (which use  $NH_4^+$  to aminate  $\alpha$ -ketoglutarate, yielding Glu) and (ii) Ala, Asp, and Tyr transaminases, all of which have Glu and pyruvate as cosubstrates and are able to catalyze the transfer of the  $-NH_2$  group from Glu into pyruvate, yielding Ala and regenerating the  $\alpha$ -ketoglutarate, as previously proposed (2, 56). Thus, Ala is a major end product of the combined glucose and amino acid metabolism. However, some data in the literature (10, 25, 58) suggest also the possible catabolism of L-Ala.

Our results indicate that L-Ala can be a “fuel for life” instead of being merely a catabolic end product to be secreted. Indeed, the presence of all enzyme activities and complexes that would be critical for enabling the complete oxidation of this amino acid to support ATP production by oxidative phosphorylation have been demonstrated: (i) L-Ala can be converted into pyruvate by different transaminases (14, 21–23, 59–61), (ii) pyruvate can be converted into acetyl-CoA and further oxidized through the tricarboxylic acid (TCA) cycle (17, 20, 25), and (iii) pyruvate can be converted into malate by the cytosolic malic enzyme—even taking into account that the reaction in the pyruvate→malate direction is very slow (36)—and further into fumarate and succinate in two subcellular compartments, the mitochondrion or the glycosomes, the peroxisome-related organelles of trypanosomatids (17, 38, 39, 62–64). All these metabolites can be used as intermediates or as fuel for the TCA cycle, thus allowing (in principle) their full oxidation (20, 25) (Fig. 5) to feed the energy metabolism. Together, our results demonstrate that extracellular L-Ala is at least partially catabolized to CO<sub>2</sub> and used for ATP production by oxidative phosphorylation. Despite the differences reported by several authors about the metabolism of this amino acid between *T. cruzi* and *Leishmania* spp. (2, 17, 38), it is tempting to stress that our results are consistent with those previously obtained with *Leishmania major* and *Leishmania braziliensis* (65–67), which also point to a complete L-Ala oxidation. Notably, the plasticity of L-Ala metabolism underlines the relevance of *T. cruzi*'s metabolic flexibility to adapt to different environmental conditions.

In conclusion, L-Ala can be produced and secreted as a main end product of the metabolism of glucose and amino acids by *T. cruzi* epimastigotes, while in the absence of glucose and at high concentrations, it can be taken up by the cells and further oxidized with production of CO<sub>2</sub>, triggering O<sub>2</sub> consumption, contributing to the maintenance of the inner mitochondrial membrane potential and powering ATP production through oxidative phosphorylation.

## MATERIALS AND METHODS

**Reagents.** L-[U-<sup>14</sup>C]Ala (0.1 mCi/ml) was purchased from American Radiolabeled Chemicals, Inc. (ARC [St. Louis, MO]). All other reagents were from Sigma (St. Louis, MO).

**Parasites.** *T. cruzi* CL strain clone 14 epimastigotes (68) were maintained in the exponential growth phase by subculture every 48 h in liver infusion tryptose (LIT). Medium supplemented with 10% fetal calf serum (FCS) at 28°C. For transport assays, exponentially growing parasites were washed three times with PBS (NaCl, 137 mM; KCl, 2.6824 mM; Na<sub>2</sub>HPO<sub>4</sub>, 8 mM; and KH<sub>2</sub>PO<sub>4</sub>, 1.4694 mM, pH 7.2) and resuspended to a final density of 2 × 10<sup>8</sup> cells/ml in PBS. To evaluate the ability of epimastigotes to use L-Ala to resist a severe metabolic stress and as an energy source, parasites in the exponential growth phase (5 × 10<sup>7</sup> parasites per ml obtained from a 24-h culture started at 2.5 × 10<sup>7</sup> parasites per ml) were washed twice in 1 volume of PBS and incubated for 30 h in 1 volume of the same buffer. After incubation, L-Ala was added to the cultures at a saturating concentration (5 mM) for its uptake, and different parameters of energy metabolism were determined, including cell viability, ATP production, oxygen consumption, and mitochondrial inner membrane potential. In all cases, the viability of the parasites was evaluated by microscopic observation of cell motility.

**Transport assays.** Transport assays were performed as described previously (40). Transport assays were initiated by the addition of 100 μl of 5 mM L-Ala in PBS to aliquots of parasites of 100 μl (2 × 10<sup>7</sup> cells each, except when otherwise specified, traced with 0.4 μCi of L-[U-<sup>14</sup>C]Ala). The uptake was measured at 28°C for 1 min, except when otherwise specified. The transport reaction was stopped by addition of 800 μl of stop solution (50 mM L-Ala in PBS, pH 7.4) prechilled at 4°C, immediately followed by two washes with cold PBS. Background values in each experiment were measured by the simultaneous addition of each traced amino acid and stop solution (29).

**Competition assays.** Competition assays were performed by measuring L-Ala uptake at a concentration equivalent to the K<sub>m</sub> in the presence of 10 times excess of each other amino acid (29). Briefly, 100-μl aliquots of parasites containing 2 × 10<sup>7</sup> cells were incubated with the transport solution supplemented with the presumably competing metabolite for 1 min. The results obtained were expressed as inhibition percentages in relation to a control (the same experiment without the competitor).

**The effect of extracellular ions, pH, and energy.** The incorporation of L-Ala in the presence of Na<sup>+</sup> and K<sup>+</sup> was measured by comparing the L-Ala uptake using a conventional PBS with the same composition as described previously, a Na<sup>+</sup>-free PBS in which all Na<sup>+</sup> was replaced by K<sup>+</sup> (149.5 mM KCl [called here Na<sup>+</sup>-free PBS]), a K<sup>+</sup>-free PBS in which all K<sup>+</sup> was replaced by Na<sup>+</sup> (149.5 mM Na<sup>+</sup> [called here K<sup>+</sup>-free PBS]), and a phosphate buffer in which the ionic strength was supplied by choline (149.5 mM choline [called here PBS-choline]) as the control. The effect of extracellular pH was determined by measuring the transport using buffers with different pHs. According to their buffer capacity,

experiments were performed using PBS for the pH range between 6.0 and 7.5, and citrate was used for the pH range between 5.0 and 6.5.

The effect of a proton-dependent plasma membrane potential on the L-Ala uptake in parasites treated with 0.5  $\mu$ M the protonophore carbonyl cyanide *p*-trifluoromethoxyphenylhydrazone (FCCP) was evaluated. As previously reported, FCCP treatment can affect an uptake process due to the disruption of the H<sup>+</sup> gradient across cellular membranes (if the uptake is performed through a H<sup>+</sup>/metabolite symporter) or to the diminution of intracellular levels of ATP due to its rapid consumption by the mitochondrial F<sub>1</sub>F<sub>o</sub>-ATP synthase, which in a low-mitochondrial-membrane-potential situation hydrolyzes ATP to pump H<sup>+</sup> to reestablish the mitochondrial inner membrane potential (40). To discriminate between both effects, a control was performed with the addition of 5  $\mu$ g/ml oligomycin A to FCCP-treated cells, which allowed simultaneous disruption of H<sup>+</sup> membrane gradients while blocking the F<sub>1</sub>F<sub>o</sub>-ATPase.

The viability of the parasites under all conditions was verified by observing their motility under the microscope.

**Analysis of data.** The disintegrations per minute (dpm) corresponding to transported radiolabeled L-Ala for each experimental point (dpm<sub>i</sub>) were calculated as dpm<sub>i</sub> = dpm<sub>e</sub> - dpm<sub>b</sub>, where dpm<sub>e</sub> is the average dpm from triplicates after 1 min of incubation in the presence of radiolabeled L-Ala and dpm<sub>b</sub> is the average dpm from the background samples.

L-Ala taken up by the cells was calculated as L-Ala<sub>i</sub> = dpm<sub>i</sub> [L-Ala]  $\nu$  dpm<sub>st</sub><sup>-1</sup> t<sup>-1</sup>, where L-Ala<sub>i</sub> is the transported L-Ala, [L-Ala] is the L-Ala nanomolar concentration,  $\nu$  is the volume of radiolabeled L-Ala, dpm<sub>st</sub> is the total dpm measured for each added radiolabeled L-Ala, and *t* is the time of incubation measured in minutes.

**Statistical analysis.** Curve adjustments, regressions, and statistical analysis were performed with the GraphPad Prism 5 analysis tools. All assays were performed at least in biological triplicate, and the details of statistical analysis were added to each figure legend.

**Estimation of number of transporters by using the Arrhenius equation.** From a thermodynamic point of view, a transporter is nothing other than a type of enzyme catalyzing, in this case, the reaction L-Ala<sub>e</sub> = >L-Ala<sub>i</sub>, where L-Ala<sub>i</sub> is the intracellular L-Ala and L-Ala<sub>e</sub> is the extracellular L-Ala.

To estimate a number of transport systems, it is necessary to measure the turnover of active sites (*k*<sub>cat</sub>). In turn, *k*<sub>cat</sub> = *V*<sub>max</sub>/no. of transporters (69).

For these systems, we proceeded to set up as a hypothesis to be tested that, at the saturated substrate concentration, the system is limited by the dissociation step. Then we can estimate the number of transporter sites at defined temperature using the Arrhenius equation as follows:

$$\text{no. of transporters} = \frac{V_{\max}}{Ae^{-\frac{E_a}{RT}}}$$

where *V*<sub>max</sub> is the maximum rate achieved by the system at saturating substrate concentration at a given temperature, *Ae* is the pre-exponential factor, *E*<sub>a</sub> is the activation energy for the reaction, *R* is the universal gas constant, and *T* is the temperature of the reaction (in kelvins).

**The contribution of L-Ala to recover cells subjected to a severe metabolic stress.** To determine whether L-Ala is able to restore the viability of epimastigotes of *T. cruzi* after a starvation period, the parasites were exponentially cultured in LIT and stressed in PBS as described above. Briefly, the epimastigotes (5 × 10<sup>7</sup> cells) were incubated for 24 and 48 h at 28°C in PBS plus 5 mM L-Ala to induce cell recovery. Separate treatments in glucose or proline were used as controls. After recovery, the cells were washed in PBS and incubated with 3-(4,5-dimethyl-2-thiazolyl)-2,5-diphenyl-2H-tetrazolium bromide (MTT) reagent to evaluate cell viability, as previously described (7).

**Mitochondrial inner membrane potential determination.** To assess the ability of L-Ala to energize the mitochondria, parasites (5 × 10<sup>7</sup> cells per ml) were starved as described above. The stressed parasites were then incubated for recovery in MCR buffer (125 mM sucrose, 65 mM KCl, 10 mM HEPES-NaOH, pH 7.2, 1 mM MgCl<sub>2</sub>, 2 mM K<sub>2</sub>HPO<sub>4</sub>) supplemented with 5 mM L-Ala or 5 mM His (positive control). Nonsupplemented MCR buffer treatment was used as negative control. Parasites were incubated with 250 nM rhodamine 123 (Sigma) for 20 min at 28°C, washed with cytomix buffer (25 mM HEPES-KOH, 120 mM KCl, 0.15 mM CaCl<sub>2</sub>, 2 mM EDTA, 5 mM MgCl<sub>2</sub>, 10 mM K<sup>+</sup>-phosphate buffer, pH 7.2, and 10  $\mu$ M FCCP if required). Changes in the fluorescence of cells labeled with rhodamine 123 were analyzed by flow cytometry. Parasites were analyzed in an FL-1 detector of a FACSCalibur flow cytometer using CellQuest Pro software (Becton, Dickinson, NJ, USA). The relative change in  $\Delta\Psi$ m was determined as the ratio between both conditions (the coupled and uncoupled states elicited by FCCP).

**ATP biosynthesis dependency of L-Ala.** To evaluate ATP production with L-Ala as their sole energy source, the parasites (approximately 5 × 10<sup>7</sup> cells per ml) were starved as described above and recovered or not (negative control) by incubation for 1 h in the presence of 5 mM His or Pro (as positive controls) or 5 mM L-Ala. The intracellular concentration of ATP in each sample was determined before and after recovery by using a luciferase assay according to the manufacturer's instructions (Sigma). ATP concentrations were estimated by using a calibration curve (ATP disodium salt, Sigma); luminescence ( $\lambda$ 570 nm) was detected using a SpectraMax i3 plate reader (Molecular Devices, Sunnyvale, CA).

**Incorporation of L-Ala into proteins.** To estimate the percentage of labeled L-Ala that was incorporated into proteins, the cells were incubated for 60 min with 5 mM L-Ala in the presence of 0.1  $\mu$ Ci of L-[U-<sup>14</sup>C]Ala. The parasites were washed twice and resuspended in 500  $\mu$ l of PBS. Then the cells were treated with 1 volume of 20% trichloroacetic acid, incubated for 1 h at room temperature, and centrifuged for 30 min at 10,000 × *g*. The pellets were resuspended in 0.1% SDS in a 15 mM Tris-HCl buffer (pH 7.4). The supernatants and pellets were resuspended in a scintillation cocktail. The amount of

radioactivity incorporated into the macromolecules was measured by a scintillation counter (PerkinElmer Tri-Carb 2910TR).

**CO<sub>2</sub> production measurements.** To measure the CO<sub>2</sub> production from the tricarboxylic acid (TCA) cycle during L-Ala catabolism, epimastigotes exponentially growing in LIT ( $5 \times 10^7$  parasites per ml) were washed twice, resuspended in PBS and incubated in 5 mM L-Ala spiked with 0.1  $\mu$ Ci of L-[U-<sup>14</sup>C]Ala for 0.5, 1, 4, and 5 h at 28°C. To trap the produced CO<sub>2</sub>, pieces of Whatman filter embedded in 2 M KOH were placed on the top of the tubes in which the parasites were incubated. The filters were recovered and mixed with scintillation cocktail, and the K<sub>2</sub><sup>14</sup>CO<sub>3</sub> production on the paper was measured by using a scintillation counter.

**Oxygen consumption.** The rates of oxygen consumption were measured using intact cells in a high-resolution oxygraph (Oxygraph-2k; Oroboros Instruments, Innsbruck, Austria). To evaluate the O<sub>2</sub> consumption rates from L-Ala, the exponentially growing parasites ( $5 \times 10^7$  cells per ml) were washed twice in PBS, subjected to nutritional stress for 16 h in the same buffer, and recovered with 5 mM L-Ala or His (positive control) for 30 min at 28°C. The parasites were added to the MCR buffer. Oligomycin A (0.5  $\mu$ g/ml) and FCCP (0.5  $\mu$ M) were sequentially added to measure the optimal noncoupled respiration and leak state of respiration, respectively. Data were recorded and treated by using DatLab 7 software.

## SUPPLEMENTAL MATERIAL

Supplemental material for this article may be found at <https://doi.org/10.1128/mSphereDirect.00338-18>.

**TEXT S1**, DOCX file, 0.02 MB.

**FIG S1**, TIF file, 0.1 MB.

**FIG S2**, TIF file, 0.1 MB.

**FIG S3**, TIF file, 0.2 MB.

**TABLE S1**, DOCX file, 0.01 MB.

## ACKNOWLEDGMENTS

This work was supported by Fundação de Amparo à Pesquisa do Estado de São Paulo grants 2016/06034-2 and 2017/16553-0 (awarded to A.M.S.), Conselho Nacional de Pesquisas Científicas e Tecnológicas (CNPq) grant 308351/2013-4 (awarded to A.M.S.), and the Research Council United Kingdom Global Challenges Research Fund under grant agreement “A Global Network for Neglected Tropical Diseases” (grant MR/P027989/1).

We are deeply indebted to Wilfredo Quiñones (Universidad de Los Andes, Mérida, Venezuela) and Paul Michels (University of Edinburgh, Edinburgh, United Kingdom) for critical reading of the manuscript.

## REFERENCES

- Lisvane Silva P, Mantilla BS, Barisón MJ, Wrenger C, Silber AM. 2011. The uniqueness of the *Trypanosoma cruzi* mitochondrion: opportunities to identify new drug target for the treatment of Chagas disease. *Curr Pharm Des* 17:2074–2099.
- Marchese L, Nascimento JF, Damasceno FS, Bringaud F, Michels PAM, Silber AM. 2018. The uptake and metabolism of amino acids, and their unique role in the biology of pathogenic trypanosomatids. *Pathogens* 7:36. <https://doi.org/10.3390/pathogens7020036>.
- Fernandes MC, Andrews NW. 2012. Host cell invasion by *Trypanosoma cruzi*: a unique strategy that promotes persistence. *FEMS Microbiol Rev* 36:734–747. <https://doi.org/10.1111/j.1574-6976.2012.00333.x>.
- Kollien AH, Schaub GA. 1998. Development of *Trypanosoma cruzi* after starvation and feeding of the vector—a review. *Tokai J Exp Clin Med* 23:335–340.
- Moreira CJ, Spata MC. 2002. Dynamics of evolution and resistance to starvation of *Triatoma vitticeps* (Reduviidae: Triatominae), submitted to two different regimens of food deprivation. *Mem Inst Oswaldo Cruz* 97:1049–1055. <https://doi.org/10.1590/S0074-02762002000700020>.
- Silber AM, Colli W, Ulrich H, Alves MJ, Pereira CA. 2005. Amino acid metabolic routes in *Trypanosoma cruzi*: possible therapeutic targets against Chagas' disease. *Curr Drug Targets Infect Disord* 5:53–64. <https://doi.org/10.2174/1568005053174636>.
- Barisón MJ, Damasceno FS, Mantilla BS, Silber AM. 2016. The active transport of histidine and its role in ATP production in *Trypanosoma cruzi*. *J Bioenerg Biomembr* 48:437–449. <https://doi.org/10.1007/s10863-016-9665-9>.
- Mantilla BS, Paes LS, Pral EM, Martil DE, Thiemann OH, Fernández-Silva P, Bastos EL, Silber AM. 2015. Role of delta1-pyrroline-5-carboxylate-dehydrogenase supports mitochondrial metabolism and host-cell invasion of *Trypanosoma cruzi*. *J Biol Chem* 290:7767–7790. <https://doi.org/10.1074/jbc.M114.574525>.
- Paes LS, Suárez Mantilla BS, Zimbres FM, Pral EM, Diogo de Melo P, Tahara EB, Kowaltowski AJ, Elias MC, Silber AM. 2013. Proline dehydrogenase regulates redox state and respiratory metabolism in *Trypanosoma cruzi*. *PLoS One* 8:e69419. <https://doi.org/10.1371/journal.pone.0069419>.
- Zeledon R. 1960. Comparative physiological studies on four species of hemoflagellates in culture. II. Effect of carbohydrates and related substances and some amino compounds on the respiration. *J Parasitol* 46:541–551. <https://doi.org/10.2307/3274935>.
- Martins RM, Covarrubias C, Rojas RG, Silber AM, Yoshida N. 2009. Use of L-proline and ATP production by *Trypanosoma cruzi* metacyclic forms as requirements for host cell invasion. *Infect Immun* 77:3023–3032. <https://doi.org/10.1128/IAI.00138-09>.
- Magdaleno A, Suárez Mantilla B, Rocha SC, Pral EM, Silber AM. 2011. The involvement of glutamate metabolism in the resistance to thermal, nutritional, and oxidative stress in *Trypanosoma cruzi*. *Enzyme Res* 2011:486928. <https://doi.org/10.4061/2011/486928>.
- Barisón MJ, Rapado LN, Merino EF, Furusho Pral EM, Mantilla BS, Marchese L, Nowicki C, Silber AM, Cassera MB. 2017. Metabolomic profiling reveals a finely tuned, starvation-induced metabolic switch in *Trypanosoma cruzi* epimastigotes. *J Biol Chem* 292:8964–8977. <https://doi.org/10.1074/jbc.M117.778522>.
- Manchola NC, Silber AM, Nowicki C. 2018. The non-canonical substrates

- of *Trypanosoma cruzi* tyrosine and aspartate aminotransferases: branched-chain amino acids. *J Eukaryot Microbiol* 65:70–76. <https://doi.org/10.1111/jeu.12435>.
15. Magdaleno A, Ahn IY, Paes LS, Silber AM. 2009. Actions of a proline analogue, L-thiazolidine-4-carboxylic acid (T4C), on *Trypanosoma cruzi*. *PLoS One* 4:e4534. <https://doi.org/10.1371/journal.pone.0004534>.
  16. Contreras VT, Salles JM, Thomas N, Morel CM, Goldenberg S. 1985. *In vitro* differentiation of *Trypanosoma cruzi* under chemically defined conditions. *Mol Biochem Parasitol* 16:315–327. [https://doi.org/10.1016/0166-6851\(85\)90073-8](https://doi.org/10.1016/0166-6851(85)90073-8).
  17. Cazzulo JJ. 1994. Intermediate metabolism in *Trypanosoma cruzi*. *J Bioenerg Biomembr* 26:157–165. <https://doi.org/10.1007/BF00763064>.
  18. Frydman B, de los Santos C, Cannata JJ, Cazzulo JJ. 1990. Carbon-13 nuclear magnetic resonance analysis of [ $^{13}\text{C}$ ]glucose metabolism in *Trypanosoma cruzi*. Evidence of the presence of two alanine pools and of two  $\text{CO}_2$  fixation reactions. *Eur J Biochem* 192:363–368. <https://doi.org/10.1111/j.1432-1033.1990.tb19235.x>.
  19. Urbina JA, Ysern X, Mildvan AS. 1990. Involvement of a divalent cation in the binding of fructose 6-phosphate to *Trypanosoma cruzi* phosphofruktokinase: kinetic and magnetic resonance studies. *Arch Biochem Biophys* 278:187–194. [https://doi.org/10.1016/0003-9861\(90\)90247-V](https://doi.org/10.1016/0003-9861(90)90247-V).
  20. Cazzulo JJ, Arauzo S, Franke de Cazzulo BM, Cannata JJB. 1988. On the production of glycerol and L-alanine during the aerobic fermentation of glucose by trypanosomatids. *FEMS Microbiol Lett* 51:187–191. <https://doi.org/10.1111/j.1574-6968.1988.tb02995.x>.
  21. Zelada C, Montemartini M, Cazzulo JJ, Nowicki C. 1996. Purification and partial structural and kinetic characterization of an alanine aminotransferase from epimastigotes of *Trypanosoma cruzi*. *Mol Biochem Parasitol* 79:225–228. [https://doi.org/10.1016/0166-6851\(96\)02652-7](https://doi.org/10.1016/0166-6851(96)02652-7).
  22. Montemartini M, Búa J, Bontempi E, Zelada C, Ruiz AM, Santomé JA, Cazzulo JJ, Nowicki C. 1995. A recombinant tyrosine aminotransferase from *Trypanosoma cruzi* has both tyrosine aminotransferase and alanine aminotransferase activities. *FEMS Microbiol Lett* 133:17–20. <https://doi.org/10.1111/j.1574-6968.1995.tb07854.x>.
  23. de Barros EG, Caldas RdA. 1983. Partial purification and characterization of glutamic-pyruvic transaminase from *Trypanosoma cruzi*. *Comp Biochem Physiol* 74:449–452.
  24. Duschak VG, Cazzulo JJ. 1991. Subcellular localization of glutamate dehydrogenases and alanine aminotransferase in epimastigotes of *Trypanosoma cruzi*. *FEMS Microbiol Lett* 67:131–135.
  25. Acosta H, Dubourdieu M, Quiñones W, Cáceres A, Bringaud F, Concepción JL. 2004. Pyruvate phosphate dikinase and pyrophosphate metabolism in the glycosome of *Trypanosoma cruzi* epimastigotes. *Comp Biochem Physiol B Biochem Mol Biol* 138:347–356. <https://doi.org/10.1016/j.cbpc.2004.04.017>.
  26. Rohloff P, Rodrigues CO, Docampo R. 2003. Regulatory volume decrease in *Trypanosoma cruzi* involves amino acid efflux and changes in intracellular calcium. *Mol Biochem Parasitol* 126:219–230. [https://doi.org/10.1016/S0166-6851\(02\)00277-3](https://doi.org/10.1016/S0166-6851(02)00277-3).
  27. Rohloff P, Montalvetti A, Docampo R. 2004. Acidocalcisomes and the contractile vacuole complex are involved in osmoregulation in *Trypanosoma cruzi*. *J Biol Chem* 279:52270–52281. <https://doi.org/10.1074/jbc.M410372200>.
  28. Rohloff P, Docampo R. 2008. A contractile vacuole complex is involved in osmoregulation in *Trypanosoma cruzi*. *Exp Parasitol* 118:17–24. <https://doi.org/10.1016/j.exppara.2007.04.013>.
  29. Silber AM, Rojas RL, Urias U, Colli W, Alves MJ. 2006. Biochemical characterization of the glutamate transport in *Trypanosoma cruzi*. *Int J Parasitol* 36:157–163. <https://doi.org/10.1016/j.ijpara.2005.10.006>.
  30. Manchola NC, Rapado LN, Barisón MJ, Silber AM. 2016. Biochemical characterization of branched chain amino acids uptake in *Trypanosoma cruzi*. *J Eukaryot Microbiol* 63:299–308. <https://doi.org/10.1111/jeu.12278>.
  31. Vanderheyden N, Benaim G, Docampo R. 1996. The role of a H(+)-ATPase in the regulation of cytoplasmic pH in *Trypanosoma cruzi* epimastigotes. *Biochem J* 318:103–109. <https://doi.org/10.1042/bj3180103>.
  32. Schnauffer A, Clark-Walker GD, Steinberg AG, Stuart K. 2005. The F1-ATP synthase complex in bloodstream stage trypanosomes has an unusual and essential function. *EMBO J* 24:4029–4040. <https://doi.org/10.1038/sj.emboj.7600862>.
  33. Maugeri DA, Cannata JJ, Cazzulo JJ. 2011. Glucose metabolism in *Trypanosoma cruzi*. *Essays Biochem* 51:15–30. <https://doi.org/10.1042/bse0510015>.
  34. Raw I. 1959. Some aspects of carbohydrate metabolism of cultural forms of *Trypanosoma cruzi*. *Rev Inst Med Trop Sao Paulo* 1:192–194.
  35. Cannata JJ, Frascó AC, Cataldi de Flombaum MA, Segura EL, Cazzulo JJ. 1979. Two forms of “malic” enzyme with different regulatory properties in *Trypanosoma cruzi*. *Biochem J* 184:409–419. <https://doi.org/10.1042/bj1840409>.
  36. Cazzulo JJ, Juan SM, Segura EL. 1977. The malic enzyme from *Trypanosoma cruzi*. *J Gen Microbiol* 99:237–241. <https://doi.org/10.1099/00221287-99-1-237>.
  37. Avilán L, García P. 1994. Hysteresis of cytosolic NADP-malic enzyme II from *Trypanosoma cruzi*. *Mol Biochem Parasitol* 65:225–232. [https://doi.org/10.1016/0166-6851\(94\)90074-4](https://doi.org/10.1016/0166-6851(94)90074-4).
  38. Haanstra JR, González-Marcano EB, Gualdrón-López M, Michels PA. 2016. Biogenesis, maintenance and dynamics of glycosomes in trypanosomatid parasites. *Biochim Biophys Acta* 1863:1038–1048. <https://doi.org/10.1016/j.bbamer.2015.09.015>.
  39. de Boiso JF, Stoppani AO. 1973. The mechanism of acetate and pyruvate oxidation by *Trypanosoma cruzi*. *J Protozool* 20:673–678. <https://doi.org/10.1111/j.1550-7408.1973.tb03596.x>.
  40. Silber AM, Tonelli RR, Martinelli M, Colli W, Alves MJ. 2002. Active transport of L-proline in *Trypanosoma cruzi*. *J Eukaryot Microbiol* 49:441–446. <https://doi.org/10.1111/j.1550-7408.2002.tb00225.x>.
  41. Harington JS. 1961. Studies of the amino acids of *Rhodnius prolixus*. I. Analysis of the haemolymph. *Parasitology* 51:309–318. <https://doi.org/10.1017/S0031182000070554>.
  42. Harington JS. 1961. Studies of the amino acids of *Rhodnius prolixus*. II. Analysis of the excretory material. *Parasitology* 51:319–326. <https://doi.org/10.1017/S0031182000070566>.
  43. Antunes LC, Han J, Pan J, Moreira CJ, Azambuja P, Borchers CH, Carels N. 2013. Metabolic signatures of triatomine vectors of *Trypanosoma cruzi* unveiled by metabolomics. *PLoS One* 8:e77283. <https://doi.org/10.1371/journal.pone.0077283>.
  44. Baydoun AR, Emery PW, Pearson JD, Mann GE. 1990. Substrate-dependent regulation of intracellular amino acid concentrations in cultured bovine aortic endothelial cells. *Biochem Biophys Res Commun* 173:940–948. [https://doi.org/10.1016/S0006-291X\(05\)80876-9](https://doi.org/10.1016/S0006-291X(05)80876-9).
  45. Bouvier LA, Silber AM, Galvão Lopes C, Canepa GE, Miranda MR, Tonelli RR, Colli W, Alves MJ, Pereira CA. 2004. Post genomic analysis of permeases from the amino acid/auxin family in protozoan parasites. *Biochem Biophys Res Commun* 321:547–556. <https://doi.org/10.1016/j.bbrc.2004.07.002>.
  46. Inbar E, Schlisselberg D, Suter Grottemeyer M, Rentsch D, Zilberstein D. 2013. A versatile proline/alanine transporter in the unicellular pathogen *Leishmania donovani* regulates amino acid homeostasis and osmotic stress responses. *Biochem J* 449:555–566. <https://doi.org/10.1042/BJ20121262>.
  47. Darling TN, Blum JJ. 1990. Changes in the shape of *Leishmania major* promastigotes in response to hexoses, proline, and hypo-osmotic stress. *J Protozool* 37:267–272. <https://doi.org/10.1111/j.1550-7408.1990.tb01145.x>.
  48. Burrows C, Blum JJ. 1991. Effect of hyper-osmotic stress on alanine content of *Leishmania major* promastigotes. *J Protozool* 38:47–52. <https://doi.org/10.1111/j.1550-7408.1991.tb04799.x>.
  49. Elliot SL, Rodrigues Jde O, Lorenzo MG, Martins-Filho OA, Guarneri AA. 2015. *Trypanosoma cruzi*, etiologic agent of Chagas disease, is virulent to its triatomine vector *Rhodnius prolixus* in a temperature-dependent manner. *PLoS Negl Trop Dis* 9:e0003646. <https://doi.org/10.1371/journal.pntd.0003646>.
  50. Cazzulo JJ, Franke de Cazzulo BM, Engel JC, Cannata JJ. 1985. End products and enzyme levels of aerobic glucose fermentation in trypanosomatids. *Mol Biochem Parasitol* 16:329–343. [https://doi.org/10.1016/0166-6851\(85\)90074-X](https://doi.org/10.1016/0166-6851(85)90074-X).
  51. Ryley JF. 1956. Studies on the metabolism of the Protozoa. 7. Comparative carbohydrate metabolism of eleven species of trypanosome. *Biochem J* 62:215–222. <https://doi.org/10.1042/bj0620215>.
  52. Chang SL. 1948. Studies on hemoflagellates; observations concerning some biochemical activities in culture, and respiration of three species of leishmanias and *Trypanosoma cruzi*. *J Infect Dis* 82:109–118. <https://doi.org/10.1093/infdis/82.2.109>.
  53. Urbina JA, Azavache V. 1984. Regulation of energy metabolism in *Trypanosoma (Schizotrypanum) cruzi* epimastigotes. II. NAD $^{+}$ -dependent glutamate dehydrogenase. *Mol Biochem Parasitol* 11:241–255. [https://doi.org/10.1016/0166-6851\(84\)90069-0](https://doi.org/10.1016/0166-6851(84)90069-0).
  54. Wynne de Martini GJ, Abramo Orrego L, de Rissio AM, Alvarez M, Mujica

- LP. 1980. Culture of *Trypanosoma cruzi* in a monophasic medium. Application to large-scale cultures in fermentation processes. *Medicina (B Aires)* 40(Suppl 1):109–114.
55. Sylvester D, Krassner SM. 1976. Proline metabolism in *Trypanosoma cruzi* epimastigotes. *Comp Biochem Physiol* 55:443–447.
56. Crispim M, Damasceno FS, Hernández A, Barisón MJ, Pretto Sauter I, Souza Pavani R, Santos Moura A, Pral EMF, Cortez M, Elias MC, Silber AM. 2018. The glutamine synthetase of *Trypanosoma cruzi* is required for its resistance to ammonium accumulation and evasion of the parasitophorous vacuole during host-cell infection. *PLoS Negl Trop Dis* 12:e0006170. <https://doi.org/10.1371/journal.pntd.0006170>.
57. Cruz-Bustos T, Potapenko E, Storey M, Docampo R. 2018. An intracellular ammonium transporter is necessary for replication, differentiation, and resistance to starvation and osmotic stress in *Trypanosoma cruzi*. *mSphere* 3:e00377-17. <https://doi.org/10.1128/mSphere.00377-17>.
58. González-Marciano E, Acosta H, Mijares A, Concepción JL. 2016. Kinetic and molecular characterization of the pyruvate phosphate dikinase from *Trypanosoma cruzi*. *Exp Parasitol* 165:81–87. <https://doi.org/10.1016/j.exppara.2016.03.023>.
59. Marciano D, Maugeri DA, Cazzulo JJ, Nowicki C. 2009. Functional characterization of stage-specific aminotransferases from trypanosomatids. *Mol Biochem Parasitol* 166:172–182. <https://doi.org/10.1016/j.molbiopara.2009.04.001>.
60. Montemartini M, Santomé JA, Cazzulo JJ, Nowicki C. 1993. Purification and partial structural and kinetic characterization of tyrosine aminotransferase from epimastigotes of *Trypanosoma cruzi*. *Biochem J* 292:901–906. <https://doi.org/10.1042/bj2920901>.
61. Nowicki C, Montemartini M, Duschak V, Santomé JA, Cazzulo JJ. 1992. Presence and subcellular localization of tyrosine aminotransferase and p-hydroxyphenyllactate dehydrogenase in epimastigotes of *Trypanosoma cruzi*. *FEMS Microbiol Lett* 71:119–124.
62. Cannata JJ, Cazzulo JJ. 1984. Glycosomal and mitochondrial malate dehydrogenases in epimastigotes of *Trypanosoma cruzi*. *Mol Biochem Parasitol* 11:37–49. [https://doi.org/10.1016/0166-6851\(84\)90053-7](https://doi.org/10.1016/0166-6851(84)90053-7).
63. Boveris A, Hertig CM, Turrens JF. 1986. Fumarate reductase and other mitochondrial activities in *Trypanosoma cruzi*. *Mol Biochem Parasitol* 19:163–169. [https://doi.org/10.1016/0166-6851\(86\)90121-0](https://doi.org/10.1016/0166-6851(86)90121-0).
64. Takashima E, Inaoka DK, Osanai A, Nara T, Odaka M, Aoki T, Inaka K, Harada S, Kita K. 2002. Characterization of the dihydroorotate dehydrogenase as a soluble fumarate reductase in *Trypanosoma cruzi*. *Mol Biochem Parasitol* 122:189–200. [https://doi.org/10.1016/S0166-6851\(02\)00100-7](https://doi.org/10.1016/S0166-6851(02)00100-7).
65. Blum JJ. 1996. Oxidation of alanine, acetate, glutamate, and succinate by digitonin-permeabilized *Leishmania major* promastigotes. *J Eukaryot Microbiol* 43:144–150. <https://doi.org/10.1111/j.1550-7408.1996.tb04495.x>.
66. Keegan FP, Sansone L, Blum JJ. 1987. Oxidation of glucose, ribose, alanine, and glutamate by *Leishmania braziliensis panamensis*. *J Protozool* 34:174–179. <https://doi.org/10.1111/j.1550-7408.1987.tb03156.x>.
67. Blum JJ. 1994. Energy metabolism in *Leishmania*. *J Bioenerg Biomembr* 26:147–155. <https://doi.org/10.1007/BF00763063>.
68. Brener Z, Chiari E. 1965. Aspects of early growth of different *Trypanosoma cruzi* strains in culture medium. *J Parasitol* 51:922–926. <https://doi.org/10.2307/3275869>.
69. Stein WD. 1989. Kinetics of transport: analyzing, testing, and characterizing models using kinetic approaches. *Methods Enzymol* 171:23–62. [https://doi.org/10.1016/S0076-6879\(89\)71006-5](https://doi.org/10.1016/S0076-6879(89)71006-5).